BioNanoSci. (2018) 8:196–206
https://doi.org/10.1007/s12668-017-0463-6

# Synergistic Antimicrobial and Cytotoxic Potential of Zinc Oxide Nanoparticles Synthesized Using *Cassia auriculata* Leaf Extract

**Hemali Padalia**[1] · **Pooja Moteriya**[1] · **Sumitra Chanda**[1]

Published online: 11 November 2017


**Abstract** The problem of microbial resistance is growing, and search for novel approaches to tackle the problem on multidrug resistance pathogens is the need of the hour. The present investigation involves green synthesis of zinc oxide nanoparticles (ZnO NPs) using *Cassia auriculata* leaf extract and evaluates its synergistic antimicrobial and cytotoxic effect. The results of various techniques confirmed the formation of ZnO NPs. UV-visible spectrum of ZnO NPs showed maximum peak at 370 nm. The crystalline nature of the ZnO NPs was confirmed by XRD analysis. The SEM analysis revealed that particles were spherical and irregular in shape, and average size of nanoparticles was 68.64 nm. The antimicrobial activity and synergistic antimicrobial activity were evaluated against pathogenic microorganisms. ZnO NPs showed broad spectrum of antimicrobial activity against tested pathogens and enhanced synergistic antimicrobial activity as compared to standard antibiotic. Cytotoxic effect of ZnO NPs was evaluated by MTT assay against HeLa cancer cell line, and ZnO NPs showed dose-dependent cytotoxic activity. The synthesized ZnO NPs possess significant antimicrobial and cytotoxic activity and hence can be used therapeutically as nanomedicine for diagnosis and drug therapy.

**Keywords** *Cassia auriculata* · Zinc oxide nanoparticles · Characterization · Synergistic antimicrobial activity · Cytotoxic activity

✉ Sumitra Chanda
svchanda@gmail.com

[1] Phytochemical, Pharmacological and Microbiological laboratory, Department of Biosciences (UGC-CAS), Saurashtra University, Rajkot, Gujarat 360005, India

## 1 Introduction

Nanotechnology is a multidisciplinary scientific field undergoing explosive development. Nanoparticles have novel optical, electronic, and structural properties that are not found in their individual molecules. Various metals have been used for synthesis of nanoparticles such as silver, gold, aluminum, zinc, carbon, titanium, iron, and copper. Metal nanoparticles have wide range of applications in the field of medicine, electronics, biosensors, biotechnology, etc. [1]. They can be synthesized by several physical and chemical methods but are not favored because of many undesirable factors like use of hazardous chemicals, lengthy and complex processes, require high temperature, pressure, and energy, and offer huge difficulties for large scale production. An attractive alternative is green synthesis, i.e., synthesis of nanoparticles with the use of plant extracts. Green methods are simple, ecofriendly, economic, nontoxic, etc. The phytoconstituents present in the plants act as reducing agents for the conversion of metals into metal nanoparticles without using any external chemicals, and thus, it becomes very environmental friendly and is the most favored method nowadays [2, 3].

Among many green-synthesized metal nanoparticles, zinc oxide nanoparticles (ZnO NPs) hold an important position. They have many applications in a wide range of fields and also possess therapeutic properties. They are used in electronics, ultraviolet light emitters, chemical sensors, personal care products, cosmetics, coating and paints, as drug carriers, etc. ZnO NPs are believed to be nontoxic, biosafe, and biocompatible and have been also used as cosmetics and in medical materials [4]. Green synthesis of ZnO NPs has been attempted for different plant species, e.g., *Pongamia pinnata* [5], *Lavandula vera* [6], *Cassia fistula* [7], *Citrullus colocynthis* [8], and *Azadirachta indica* [9].

*Cassia auriculata* L. commonly known as awal is a shrub belonging to Fabaceae family. It is widely used in traditional medicine for rheumatism, conjunctivitis, and diabetes. Leaves and fruits as an anthelmintic root used for skin diseases and seeds were used for treatment of eye infection [10]. The antimicrobial and antioxidant property of *C. auriculata* leaves and stem extracts is reported by Chanda et al. [11]. Silver nanoparticles synthesized using the *C. auriculata* flower is showed significant catalytic activity is reported by Muthu and Priya [12]. The aim of the present study was to synthesize ZnO NPs using *Cassia auriculata* leaf aqueous extract and evaluate the synergistic antimicrobial and cytotoxic activity of ZnO NPs.

## 2 Materials and Methods

### 2.1 Plant Materials and Chemicals

Fresh leaves of *Cassia auriculata* were collected from Rajkot, Gujarat, India. All the chemicals were obtained from HiMedia Laboratories Pvt. Ltd., Mumbai, India. Ultra-purified water was used for all the experiments.

### 2.2 Preparation of the Plant Extract

Fresh leaves of *Cassia auriculata* were thoroughly washed with tap water followed by ultra-purified water and dried under shade. The dried plants were homogenized to fine powder and stored in airtight bottles. Five grams of leaf powder was taken in a 250-ml glass beaker along with 100 ml ultra-purified water and placed it on a magnetic stirrer at a temperature of 80 °C for 1 h. The extract was cooled to room temperature and filtered through Whatman No.1 filter paper. The filtered extract was used for the synthesis of ZnO NPs.

### 2.3 Synthesis of Zinc Oxide Nanoparticles

Zinc oxide nanoparticles were synthesized using the procedure as described by Padalia and Chanda [13]. Fifty milliliters of leaf extract was taken in a beaker and heated at 80 °C on a magnetic stirrer heater. Five grams of zinc nitrate ($ZnNO_3$) was then added to the leaf extract when the temperatures reached 80 °C. The mixture was heated until it was reduced to a deep yellow color paste. The paste was collected in a ceramic crucible and heated in a Muffle Furnace at 400 °C for 2 h. A light yellow color powder of ZnO NPs was obtained which was carefully collected and stored at 4 °C for further analysis.

### 2.4 Characterization of the Zinc Oxide Nanoparticles

Characterization of the synthesized ZnO NPs was carried out by various spectroscopy techniques like UV-Vis spectroscopy, zeta potential, thermal gravimetric analysis (TGA), fourier transform infrared (FTIR) spectroscopy, X-ray diffraction analysis (XRD), and scanning electron microscopy (SEM) analysis as described by Padalia et al. [14].

### 2.5 Antimicrobial Activity

The antimicrobial potential of ZnO NPs was evaluated against four Gram-positive bacteria (*Bacillus cereus* (BC) ATCC11778, *Bacillus subtilis* (BS) ATCC6633, *Staphylococcus aureus* (SA) ATCC29737, *Corynebacterium rubrum* (CR) ATCC14898), four Gram-negative bacteria (*Escherichia coli* (EC) NCIM2931, *Pseudomonas aeruginosa* (PA) ATCC9027, *Klebsiella pneumoniae* (KP) NCIM2719, and *Salmonella typhimurium* (ST) ATCC23564), and three fungi (*Cryptococcus neoformans* (CN) ATCC34664, *Candida albicans* (CA) ATCC2091, and *Candida glabrata* (CG) NCIM3438). The microorganisms were obtained from National Chemical Laboratory, Pune, India. The microorganisms were maintained at 4 °C.

#### *2.5.1 Agar Well Diffusion Assay*

In vitro antimicrobial activity of ZnO NPs was determined by agar well diffusion assay [15]. Molten Mueller Hinton agar/Sabouraud dextrose agar (40–42 °C) was seeded with 200 μl of inoculums ($1 \times 10^8$ cfu/ml) and poured into petri dishes. The media was allowed to solidify, and wells were prepared in the seeded agar plates with the help of a cup borer (8.5 mm). Five different concentrations (25, 50, 75, 100, and 150 mg/ml) of ZnO NPs were made in 100% DMSO; 100 μl of different concentrations of nanoparticles was added into the well. The plates were incubated at 37 and 28 °C for 24 and 48 h for bacteria and fungi, respectively. DMSO was used as a negative control. Antimicrobial activity was assayed by measuring the diameter of the zone of inhibition formed around the well in millimeters. The experiment was done in triplicate, and the average values were calculated for antimicrobial activity.

### 2.6 Synergistic Activity

The synergistic antimicrobial activity of synthesized ZnO NPs was evaluated with 15 standard antibiotics. The antimicrobial activity of ZnO NPs alone, antibiotics alone, and ZnO NPs plus antibiotics was determined against four Gram-positive bacteria, four Gram-negative bacteria, and three fungal strains by agar disc diffusion method.

#### *2.6.1 Antibiotics Used in the Study*

All the antibiotics were purchased from HiMedia Laboratories Pvt. Ltd., Mumbai, India. Antibiotics used in the study were

cefpirome ($CFP^{30}$), cephalothin ($CEP^{30}$), gentamicin ($GEN^{10}$), amoxyclav ($AMC^{10}$), chloramphenicol ($C^{30}$), amikacin ($AK^{10}$), tetracycline ($TE^{30}$), polymyxin B ($PB^{100}$), ampicillin ($AMP^{10}$), ketoconazole ($KT^{30}$), itraconazole ($IT^{30}$), clotrimazole ($CC^{10}$), fluconazole ($FLC^{10}$), amphotericin B ($AP^{100}$), and nystatin ($NS^{100}$).

*2.6.2 Agar Disc Diffusion Assay*

Synergistic antimicrobial activity of ZnO NPs with all antibiotics was evaluated by using agar disc diffusion method [16]. The petri plates were prepared by pouring 20 ml molten Mueller Hinton agar/Sabouraud dextrose agar seeded with 200 μl test culture containing $1 \times 10^8$ cfu/ml as McFarland 0.5 turbidity standard. Plates were allowed to solidify. Standard antibiotic paper discs (6 mm) were impregnated with 20 μl of ZnO NPs (5 mg/ml) dissolved in DMSO. All the discs were allowed to saturate for 30 min and were placed on the surface of the agar plates which had previously been inoculated with microorganisms. All plates were incubated for 24 and 48 h at 37 and 28 °C for bacteria and fungi, respectively. Results were recorded by measuring the zone of inhibition appearing around the discs. All the tests were performed in triplicate and the mean values are presented.

**Increase in Fold Area** Increase in fold area (IFA) was calculated by using the formula of Gajhiye et al. [17].

$$\left(b^2 - a^2\right)/a^2$$

where $a$ is the zone of inhibition of antibiotics and $b$ is the zone of inhibition of ZnO NPs + antibiotics.

### 2.7 In Vitro Cytotoxic Activity

Cancer cell viability of the ZnO NPs was evaluated by the MTT (3-[4,5-dimethylthiazol-2-yl]-2,5-diphenyltetrazolium bromide) assay against HeLa cancer cell line [18, 19]. One hundred fifty microliters of HeLa cells was seeded in the 96-well plates (Becton Dickinson (BD), USA) at the density of $4 \times 10^4$ viable cells/well (HeLa) and incubated 24 h to allow cell attachment. Following attachment, the medium was replaced with complete medium (150 μl/well) containing the ZnO NP concentrations ranging from 2 to 200 μg/ml for 72 h. Following treatment, the cells were washed with PBS and incubated with 100 μl/well fresh medium containing 0.5 mg/ml MTT. The MTT-containing medium was removed after 3 h incubation in dark condition. The MTT formazan was dissolved in 100 μl/well. DMSO and optical density were determined at 570 nm using an ELISA plate reader (Bio-Tek, USA). Standard anticancer drug mitomycin C was used as a positive control. Cell viability was calculated by the following equation:

$$Cell\ viability\ (\%) = (A_S/A_{Control}) \times 100$$

where $A_s$ is the absorbance of the cells incubated with ZnO NPs and leaf extract, and $A_{control}$ is the absorbance of the cells incubated with the culture medium only.

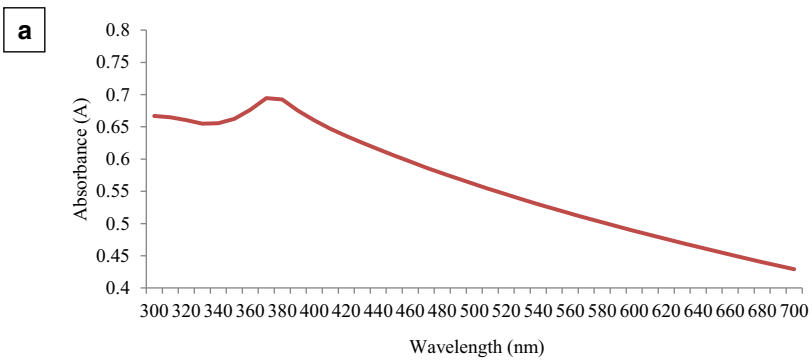


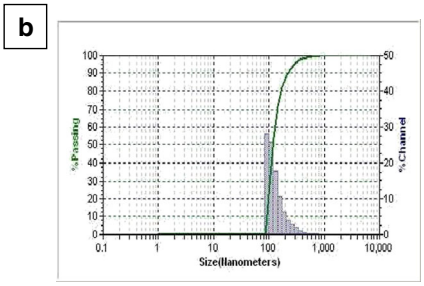


| | |
|---|---|
| Zeta potential | 16.63 mv |
| Charge | 0.537 Fc |
| Polarity | Positive |
| Mobility | 1.30u/ s/ V/ cm |
| Conductivity | 277 uS/cm |

**Fig. 1** **a** UV-Vis spectrum and **b** zeta potential of ZnO NPs

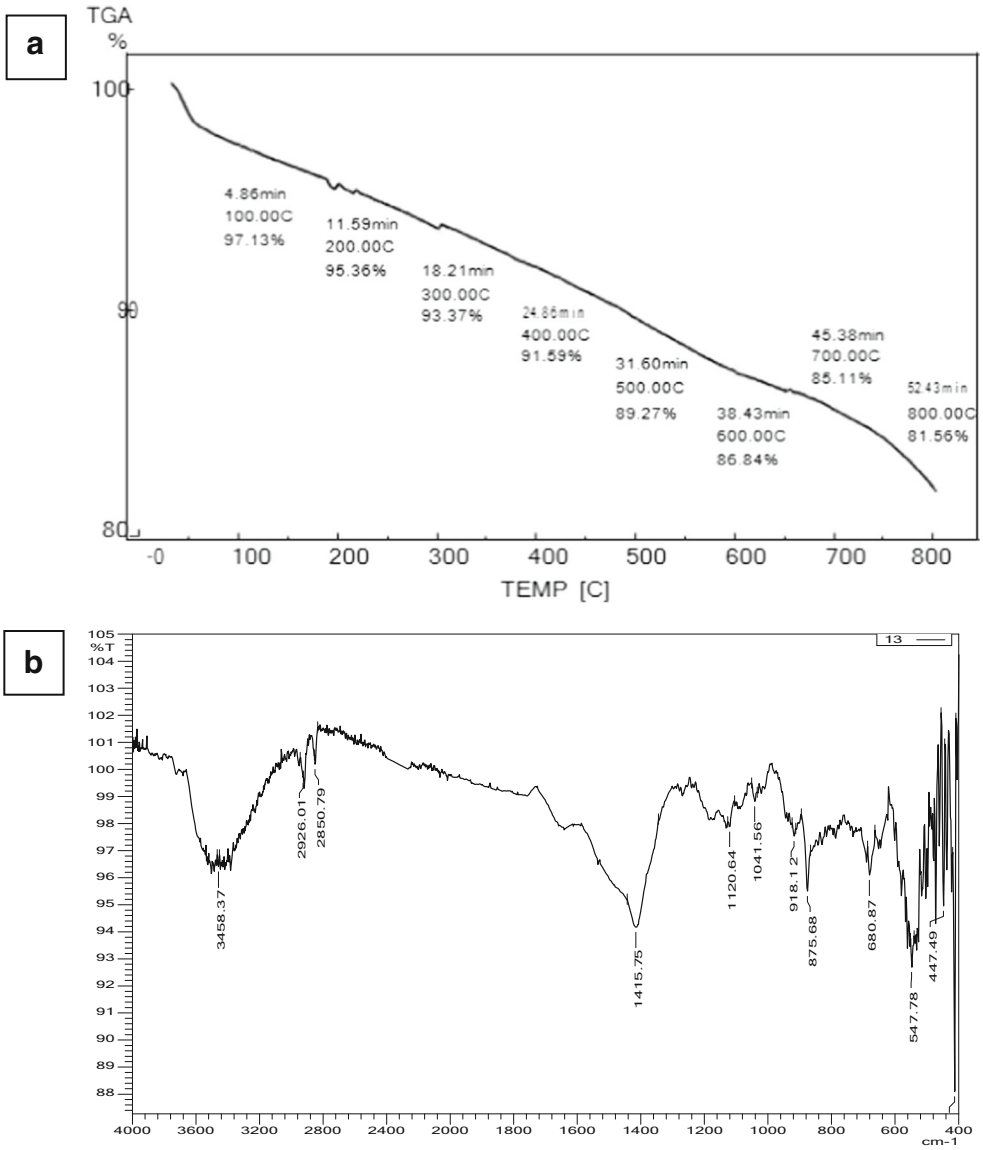


**Fig. 2** **a** Thermal gravimetric curve and **b** FTIR spectrum of ZnO NPs

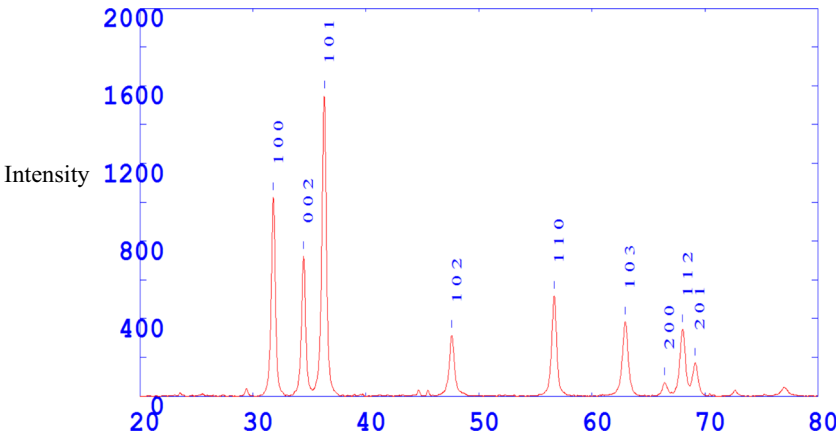


**Fig. 3** XRD pattern of ZnO NPs

## 3 Results and Discussion

### 3.1 UV-visible Spectroscopy and Zeta Potential Analysis

UV-Vis spectroscopy serves as a preliminary tool to confirm the formation of nanoparticles. The synthesized ZnO NPs showed strong absorbance peak at 370 nm due to its surface plasmon resonance (Fig. 1a); this result confirmed the formation of ZnO NPs synthesized from the leaf extract of *Cassia auriculata*. Vijayakumar et al. [20] reported that ZnO NPs synthesized using *Plectranthus amboinicus* leaf extract showed absorbance peak at 375 nm. The surface charge of synthesized ZnO NPs was 16.63 mv determined by zeta potential (Fig. 1b). This suggested that nanoparticles were positively charged and stable.

### 3.2 Thermal Gravimetric Analysis

The thermal gravimetric curve of green-synthesized ZnO NPs is shown in Fig. 2a. TGA spectrum showed the significant weight loss of ZnO NPs when heated from 0 to 800 °C. The initial weight loss observed at 200 °C was 4.64% which is ascribed the removal of water molecules on the surface of ZnO NPs. Thereafter, the gradual weight loss observed up to 800 °C was 18.45% which is due to thermal degradation of plant bioorganic molecules absorbed on ZnO NPs. Ramesh et al. [21] also reported thermal decomposition of ZnO NPs synthesized by *Solanum nigrum* leaf extracts.

### 3.3 Fourier Transform Infrared Spectroscopy

FTIR spectroscopy is used to identify the possible functional groups responsible for capping and efficient stabilization of ZnO NPs. FTIR spectrum of synthesized ZnO NPs is given in Fig. 2b. The absorption band at 3458.37 $cm^{-1}$ is the characteristics of the O-H stretching of alcohol group. The absorption band at 2926.01 and 2850.79 $cm^{-1}$ corresponds to the C-H stretching of alkane group. The absorption band at 1041.56 $cm^{-1}$ indicates C-O stretching of ether group. The absorption peak at 918.12, 875.68, and 680.87 $cm^{-1}$ shows =C-H bending of alkene group. The absorption band at 547.78 $cm^{-1}$ indicates C-R stretching of alkyl halide group.

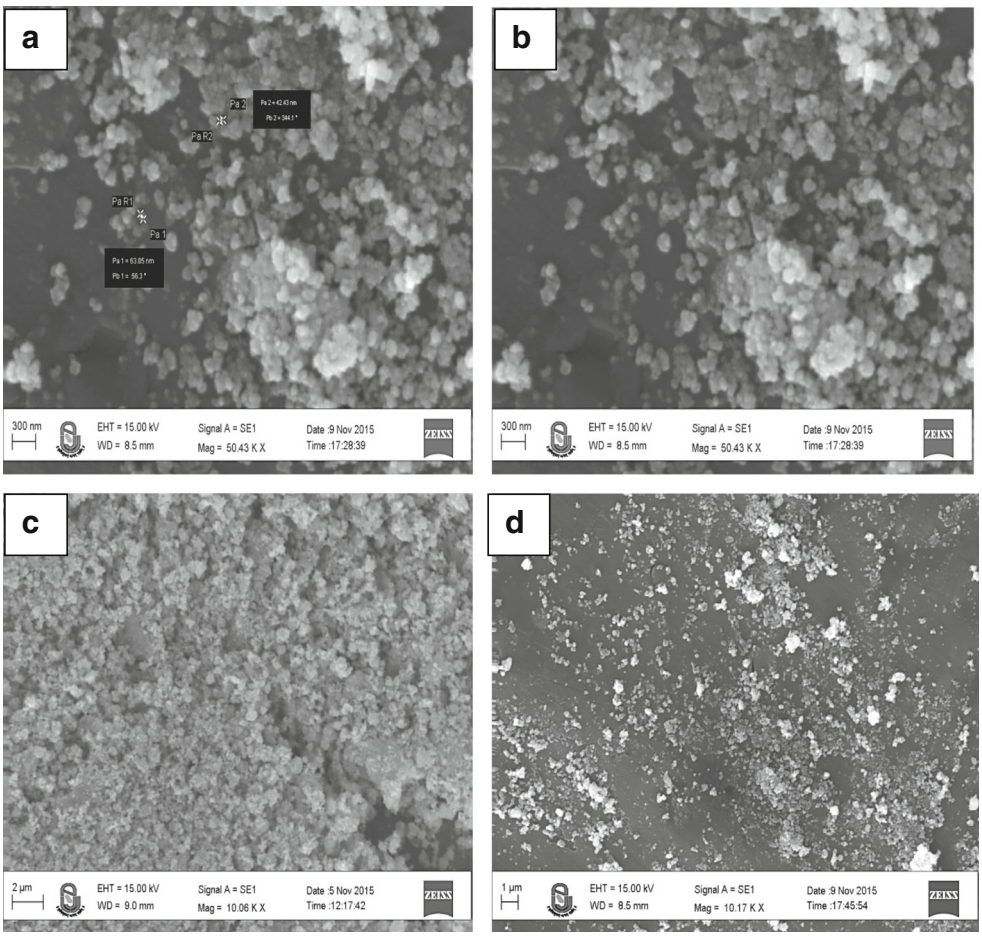


**Fig. 4** **a**–**d** SEM images of ZnO NPs at different magnifications

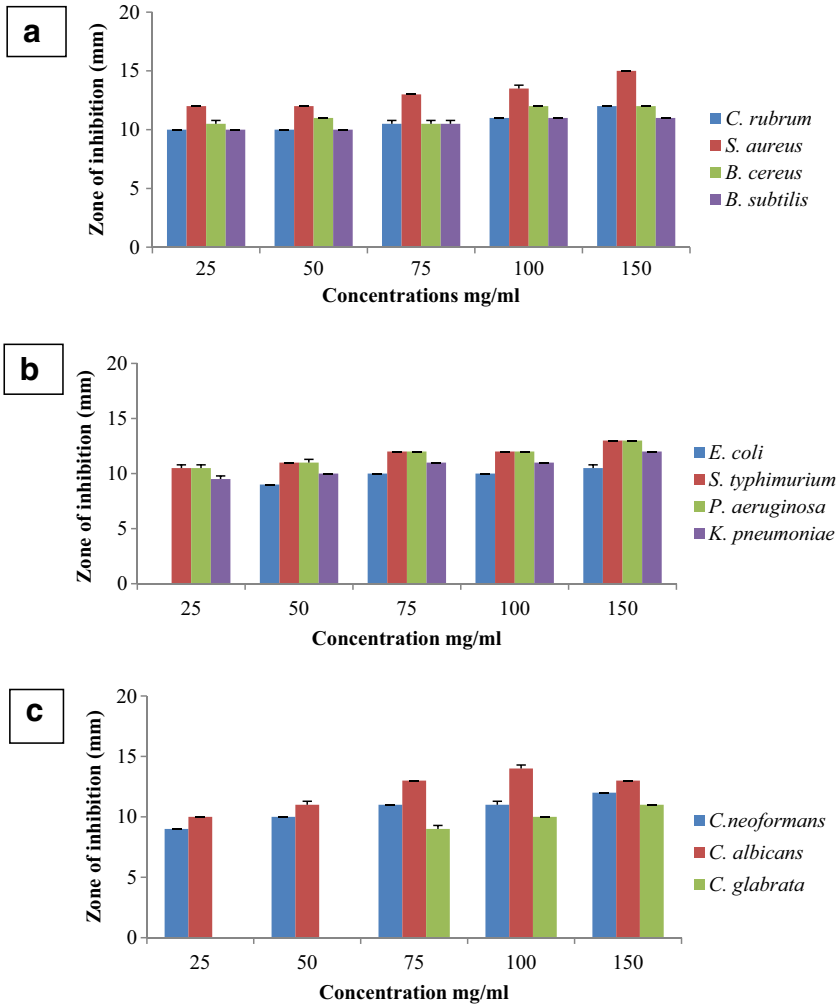


**Fig. 5** Antimicrobial activity of ZnO NPs against **a** Gram-positive bacteria, **b** Gram-negative bacteria, and **c** Fungi

**Table 1** Synergistic activity of ZnO NPs with different commercial antibiotics against Gram-positive bacteria

| Antibiotic | *B. subtilis* | | | *B. cereus* | | | *C. rubrum* | | | *S. aureus* | | |
|---|---|---|---|---|---|---|---|---|---|---|---|---|
| | AB (*a*) | AB + ZnO NPs (*b*) | IFA | AB (*a*) | AB + ZnO NPs (*b*) | IFA | AB (*a*) | AB + ZnO NPs (*b*) | IFA | AB (*a*) | AB + ZnO NPs (*b*) | IFA |
| $CFP^{30}$ | 9 | 15 | 1.77 | – | – | – | 8 | 7.5 | – | 9 | – | – |
| $CEP^{30}$ | 20.5 | 22 | 0.15 | 30 | 45 | 1.25 | 17.5 | 49.5 | 7.00 | 15.5 | 20 | 0.66 |
| $GEN^{10}$ | 9.5 | 13.5 | 1.09 | 35 | 40.5 | 0.33 | 8.5 | 40.5 | 21.70 | 9 | 11 | 0.49 |
| $AMC^{10}$ | 10.5 | 12 | 0.30 | 8 | 12 | 1.25 | 13 | 18.5 | 1.02 | 13 | 14.5 | 0.24 |
| $C^{30}$ | 15 | 17 | 0.28 | 34.5 | 29.5 | – | 9.5 | 34 | 11.80 | 8 | 11 | 0.89 |
| $AK^{10}$ | 9.5 | 12.5 | 0.73 | 37.5 | 35.5 | – | 34 | 43.5 | 0.63 | – | – | – |
| $TE^{30}$ | 14.5 | 18.5 | 0.62 | 20.5 | 38 | 2.43 | 40 | 43.5 | 0.18 | 14.5 | 16.5 | 0.29 |
| $PB^{100}$ | 9.5 | 10.5 | 0.22 | 12 | 17.5 | 1.12 | 8 | 22.5 | 6.91 | 8 | 10 | 0.56 |
| $AMP^{10}$ | 10 | 11.5 | 0.32 | 9 | 12 | 0.77 | 19 | 24 | 0.59 | 17 | 17 | – |

*AB* antibiotic, *IFA* increase in fold area. Mean surface area of the zone of inhibition was calculated for each from the mean diameter. Increase in fold area was calculated as $b^2 - a^2/a^2$, where $a$ is the inhibition zones for antibiotics and $b$ is the inhibition zones for antibiotics + ZnO NPs, respectively. All values are express in mm

Antibiotics: cefpirome ($CFP^{30}$), cephalothin ($CEP^{30}$), gentamicin ($GEN^{10}$), amoxyclav ($AMC^{10}$), chloramphenicol ($C^{30}$), amikacin ($Ak^{10}$), tetracycline ($TE^{30}$), polymyxin B ($PB^{100}$), and ampicillin ($AMP^{10}$)

**Table 2** Synergistic activity of synthesized ZnO NPs with different commercial antibiotics against Gram-negative bacteria

| Antibiotic | *E. coli* | | | *S. typhimurium* | | | *P. aeruginosa* | | | *K. pneumoniae* | | |
|---|---|---|---|---|---|---|---|---|---|---|---|---|
| | AB (*a*) | AB + ZnO NPs (*b*) | IFA | AB (*a*) | AB + ZnO NPs (*b*) | IFA | AB (*a*) | AB + ZnO NPs (*b*) | IFA | AB (*a*) | AB + ZnO NPs (*b*) | IFA |
| $CFP^{30}$ | 13 | 14 | 0.15 | 22 | 14.5 | – | 9.5 | 9.5 | – | 12.5 | 9.5 | – |
| $CEP^{30}$ | 10 | 10 | – | 22.5 | 19 | – | 38.5 | 39.5 | 0.05 | 40.5 | 39.5 | – |
| $GEN^{10}$ | 17 | 19.5 | 0.31 | 23 | 20.5 | – | 15.5 | 28 | 2.26 | 17.5 | 28 | 1.56 |
| $AMC^{10}$ | 13 | 13 | – | 24 | 16 | – | 10.5 | 9 | – | 22 | 9 | – |
| $C^{30}$ | 14.5 | 21 | 1.09 | 27.5 | 27.5 | – | 10.5 | 10 | – | 31 | 10 | – |
| $AK^{10}$ | 15.5 | 20.5 | 0.74 | 27.5 | 23 | – | 16 | 22.5 | 0.97 | 29 | 22.5 | – |
| $TE^{30}$ | 16.5 | 20 | 0.46 | 25 | 27 | 0.16 | 20 | 22 | 0.21 | 41 | 22 | – |
| $PB^{100}$ | 11 | 11.5 | 0.092 | 11 | 13.5 | 0.50 | 10.5 | 10.5 | – | 11 | 10.5 | – |
| $AMP^{10}$ | 19.5 | 16.5 | – | 30 | 25.5 | – | 17 | 12 | – | 30.5 | 12 | – |

*AB* antibiotic, *IFA* increase in fold area. Mean surface area of the zone of inhibition was calculated for each from the mean diameter. Increase in fold area was calculated as $b^2 - a^2/a^2$, where *a* is the inhibition zones for antibiotics and *b* is the inhibition zones for antibiotics + ZnO NPs, respectively. All values are express in mm

Antibiotics: cefpirome ($CFP^{30}$), cephalothin ($CEP^{30}$), gentamicin ($GEN^{10}$), amoxyclav ($AMC^{10}$), chloramphenicol ($C^{30}$), amikacin ($Ak^{10}$), tetracycline ($TE^{30}$), polymyxin B ($PB^{100}$), and ampicillin ($AMP^{10}$)

This band indicates involvement of phytoconstituent present in *Cassia auriculata* leaf extract having functional groups of alkene, alcohol, ether, and alkane in reduction and stabilization of ZnO NPs. Similar results were reported by Awwad et al. [22] and Nagajyothi et al. [23] for ZnO NPs synthesized using *Olea europea* leaf and *Polygala tenuifolia* root extracts, respectively.

### 3.4 X-ray Diffraction Analysis

X-ray diffraction analysis is use to confirm nature of ZnO NPs. The X-ray diffraction patterns of synthesized ZnO NPs are given in Fig. 3. XRD spectrum of synthesized ZnO NPs were showed the peaks at 2θ of 31.814°, 34.495°, 36.318°, 47.600°, 56.654°, 62.940°, 66.423°, 68.029°, and 69.116° could be attributed to the 100, 002, 101, 102, 110, 103, 200, 112, and 201 planes, respectively. All of the diffraction peaks confirm the hexagonal wurtzite structure of ZnO NPs (JCPDS card no. 36-1451). The sharp strong and narrow diffraction intense peaks indicate that the synthesized ZnO NPs are highly crystalline. Nair et al. [24] also reported that the peaks were recognized as 100, 002, 102, 110, 103, and 112 reflections in synthesized ZnO NPs.

### 3.5 Scanning Electron Microscopy Analysis

The SEM images of ZnO NPs at different magnification of 10.05, 30.25, and 40.06 K are depicted in Fig. 4(a-d). The

**Table 3** Synergistic activity of synthesized ZnO NPs with different commercial antibiotics against fungi

| Antibiotic | *C. albicans* | | | *C. glabrata* | | | *C. neoformans* | | |
|---|---|---|---|---|---|---|---|---|---|
| | AB (*a*) | AB + ZnO NPs (*b*) | IFA | AB (*a*) | AB + ZnO NPs (*b*) | IFA | AB (*a*) | AB + ZnO NPs (*b*) | IFA |
| $KT^{30}$ | 16 | 18.5 | 0.33 | 26 | 21 | – | 15.5 | 27 | 2.03 |
| $IT^{30}$ | 9.5 | 10 | 0.10 | 19.5 | 15 | – | 18 | 18.5 | 0.05 |
| $CC^{10}$ | – | 10 | – | 14.5 | 13 | – | 15.5 | 20 | 0.66 |
| $FLC^{10}$ | 17 | 18.5 | 1.83 | 14 | – | – | 13.5 | 23.5 | 2.03 |
| $AP^{100}$ | 8.5 | 10 | 0.38 | 13.5 | 10 | – | 12.5 | 11.5 | – |
| $NS^{100}$ | 15.5 | 17 | 0.20 | 28.5 | 16 | – | 22.5 | 21 | – |

*AB* antibiotic, *IFA* increase in fold area. Mean surface area of the zone of inhibition was calculated for each from the mean diameter. Increase in fold area was calculated as $b^2 - a^2/a^2$, where *a* is the inhibition zones for antibiotics and *b* is the inhibition zones for antibiotics + ZnO NPs, respectively. All values are express in mm

Ketoconazole ($KT^{30}$), itraconazole ($IT^{30}$), clotrimazole ($CC^{10}$), fluconazole ($FLC^{10}$), amphotericin B ($AP^{100}$), nystatin ($NS^{100}$)

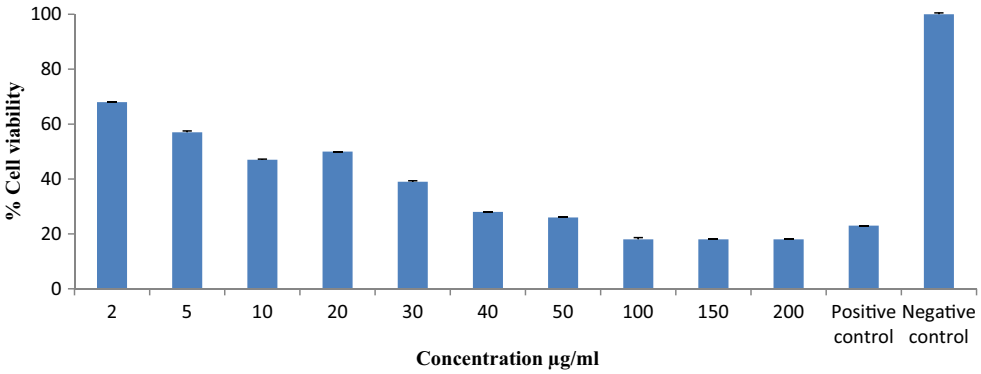


**Fig. 6** Cytotoxic effect of ZnO NPs against HeLa cells

ZnO NPs were found to be predominantly spherical and irregular in shape. The average particle size of ZnO NPs was 68.64 nm. Rao et al. [25] also reported the average particle size of ZnO NPs 63.4 nm synthesized using *Aloe vera* extract. Spherical shape of ZnO NPs synthesized from various plant extracts is also reported by other researches [26, 27].

### 3.6 Antimicrobial Activity

The antimicrobial activity of ZnO NPs was evaluated with five different concentrations (25, 50, 75, 100, and 150 mg/ml) against four Gram-positive bacteria, four Gram-negative bacteria, and three fungi is given in Fig. 5. All the five concentrations of ZnO NPs inhibited all the four Gram-positive bacteria, but inhibitory activity was more against *S. aureus* and *C. rubrum*. Concentration-dependent inhibitory activity was observed against both these bacteria while both *Bacillus* strains (*B. cereus* and *B. subtilis*) were not affected by increased concentration of ZnO NPs, though higher concentration of ZnO NPs showed slightly more activity (Fig. 5a). Maximum antibacterial activity was against *S. aureus*. Janaki et al. [28] also found that synthesized ZnO NPs by green route were showed higher antimicrobial activity against Gram-positive bacteria *S. aureus*.

No clear cut concentration effect was found against all the four Gram-negative bacteria, but definitely, higher concentration showed slightly more inhibition than lower concentration. All four Gram-negative bacteria were equally inhibited; however, the activity was lower than Gram-positive bacteria (Fig. 5b). Differential inhibition of Gram-positive and Gram-negative bacteria is due to difference in the cell wall composition of both bacteria [29, 30]. Madan et al. [9] also reported that ZnO NPs effectively inhibit the growth of Gram-positive bacteria than Gram-negative bacteria.

The fungi *C. neoformans* and *C. albicans* were inhibited by all the five concentrations of ZnO NPs while *C. glabrata* was inhibited by only higher concentration of ZnO NPs (Fig. 5C). The antifungal activity against *C. albicans* was more than *C. neoformans*. On the whole, antibacterial activity was more than antifungal activity. Green-synthesized ZnO NPs showed different levels of antimicrobial activity against different pathogens as reported by several researchers. Sharma [31] also reported effective antibacterial activity of ZnO nanoflowers synthesized using *Carica papaya* milk against *Pseudomonas aeruginosa*, *Staphylococcus aureus*, *Klebsiella aerogenes*, and *Pseudomonas desmolyticum* strains and most susceptible bacterial pathogen was *Pseudomonas aeruginosa*. Jayaseelan et al. [32] also observed the significant antimicrobial activity of ZnO NPs against *Pseudomonas aeruginosa* and *Aspergillus flavus*.

### 3.7 Synergistic Antimicrobial Activity

The synergistic antimicrobial activity of ZnO NPs was evaluated with 15 standard antibiotics against four Gram-positive bacteria, four Gram-negative bacteria, and three fungi. The increase in fold area of synthesized ZnO NPs with antibiotics against Gram-positive bacteria is given in Table 1.The antibiotics $CFP^{30}$, $TE^{30}$, $GEN^{10}$, and $C^{30}$ had the highest increase in fold area 1.77, 2.43, 21.70, and 0.89 against *B. subtilis*, *B. cereus*, *C. rubrum*, *and S. aureus*, respectively. ZnO NPs plus all nine antibiotics showed more synergistic activity than antibiotics alone against *B. subtilis*.

The increase in fold area of synthesized ZnO NPs with antibiotics against Gram-negative bacteria is given in Table 2. The antibiotics $C^{30}$, $PB^{100}$, and $GEN^{10}$ had the highest increase in fold area 1.09, 0.50, and 2.26 against *E. coli*, *S. typhimurium*, and *P. aeruginosa*, respectively. There was no increase in fold area with eight antibiotics against *K. pneumoniae* except $GEN^{10}$ (1.56). Banoee et al. [33] also found that ZnO NPs combined with ciprofloxacin had enhanced antibacterial activity against *E. coli* and *S. aureus*. Dobrucka and Dugaszewska [34] also reported that ZnO NPs with gentamicin showed better antibacterial activity against *P. aeruginosa.*

The increase in fold area of synthesized ZnO NPs with antibiotics against fungi is given in Table 3. The antibiotics $FLC^{10}$ had the highest increase in fold area 1.83 against *C. albicans* while antibiotics $FLC^{10}$ and $KT^{30}$ had the highest increase in fold area 2.03 against *C. neoformans*. There was

no increase in fold area with any of the antibiotics against *C. glabrata*.

ZnO NPs alone did not show antimicrobial activity but in combination with standard antibiotics showed strong synergistic antimicrobial activity. The increase in synergistic antimicrobial effect may be caused by the reaction between nanoparticles and antibiotics. The organic antimicrobials contain many active groups such as hydroxyl and amido groups, which can coordinate easily with metal nanoparticles by chelation [35]. AbdElhady [36] reported that ZnO NPs combined with antibiotics showed enhanced antibacterial activity compared with uncombined ZnO NPs. Sharma et al. [37] reported 100% synergistic antimicrobial activity of zinc oxide nanoparticles with antibiotics ciprofloxacin and ampicillin.

The present results suggest that *Cassia* leaf synthesized ZnO NPs showed more antibacterial activity than antifungal activity. The antimicrobial activity depicted by synthesized ZnO NPs may be because of combination of more than one reason. Formation of reactive oxygen species like SO, $OH^-$, $H_2O_2$, and $O_2^{2-}$ which might have distorted and damaged the bacterial cell membrane, resulting in the leakage of intracellular contents and eventually the death of bacterial cell [38]. The deposition or accumulation of ZnO NPs on the surface of bacteria or either in the cytoplasm or in the periplasmic region of cell leads to damage of the membrane of the bacteria and results in cell death [39]. Smaller particle size provides relatively large surface area to volume ratio that triggers toxicity effect of ZnO NPs towards the bacteria [40].

### 3.8 In Vitro Cytotoxic Activity

The cytotoxic activity of ZnO NPs against HeLa cancer cell line was examined in terms of percentage cell viability by MTT assay is given in Fig.6. ZnO NPs showed dose-dependent cytotoxic activity, as concentration of ZnO NPs increased, percentage cell viability decreased. Even at very low concentration of ZnO NPs i.e., at 2 μg/ml, the cell viability was 68% i.e., cytotoxic effect was evident. At 50 μg/ml concentration, the standard drug mitomycin C resulted in 23% cell viability, and at the same concentration, the synthesized ZnO NPs resulted in 26% cell viability. Negative control without nanoparticles showed 100% cell viability. The cytotoxic effect of synthesized ZnO NPs was as good as that of standard drug. Dose-dependent cytotoxic effect of ZnO NPs was observed against Hep-G2 cell line by Chung et al. [41] and against HeLa cell line by Padalia and Chanda [13]. Nanoparticles induce cell death through reactive oxygen species generation and activation of an integrated cytotoxic pathway that includes mitochondrial depolarization and plasma membrane leakage [42]. This study suggested the use of ZnO NPs as a new method to combat diseases like cancer due to their potential cytotoxic effect and ability to inhibit the growth of cancer cells.

## 4 Conclusion

Green synthesis of ZnO NPs using *Cassia auriculata* leaf extract is low cost, ecofriendly, and simple. The reduction of zinc ions by *Cassia auriculata* leaf extract resulted in the formation of stable nanoparticles. The optical absorbance peak was recorded at 370 nm confirms the formation of ZnO NPs. SEM analysis demonstrated that ZnO NPs are spherical and irregular in shape and average particle size is 68.64 nm. ZnO NPs showed broad spectrum of antimicrobial activity and also exhibited better synergistic antimicrobial activity as compared to standard antibiotics. Synthesized ZnO NPs showed potent cytotoxic effect against HeLa cancer cell lines. Hence, this green-synthesized ZnO NPs can be effectively used as potential antimicrobial agent to inhibit various microbial pathogens and has a great potential in the preparation of drugs used as a novel medicine in therapeutic application in disease like cancer.

**Acknowledgements** The authors thank the Department of Biosciences (UGC-CAS) for providing excellent research facilities. Ms. Hemali Padalia is thankful to UGC-CAS, and Ms. Pooja Moteriya is thankful to UGC, New Delhi, India, for providing Junior Research Fellowship.

**Compliance with Ethical Standards**

**Conflict of Interest** The authors declare that they have no conflict of interest.

## References

1. West, J. L., & Halas, N. J. (2000). Applications of nanotechnology to biotechnology: commentary. *Current Opinion in Biotechnology, 11*(2), 215–217.
2. Mason, C., Vivekanandha, S., Misra, M., & Mohanty, A. K. (2012). Switch grass (*Panicum virgatum*) extract medicated green synthesis of silver nanoparticles. *World Journal of Nano Science and Engineering, 2*, 47–52.
3. Devi, R. S., & Gayathri, R. (2014). Green synthesis of zinc oxide nanoparticles by using *Hibiscus rosa-sinensis*. *International Journal of Current Engineering and Technology, 4*(4), 2444–2446.
4. Wang, Z. L. (2004). Zinc oxide nanostructures: growth, properties and applications. *Journal of Physics: Condensed Matter, 16*(25), 829–858.
5. Malaikozhundan, B., Vaseeharan, B., Vijayakumar, S., Pandiselvi, K., Kalanjiam, M. A. R., Murugan, K., & Benelli, G. (2017). Biological therapeutics of *Pongamia pinnata* coated zinc oxide nanoparticles against clinically important pathogenic bacteria, fungi and MCF-7 breast cancer cells. *Microbial Pathogenesis, 104*, 268–277.
6. Salari, Z., Ameri, A., Forootanfar, H., Adeli-Sardou, M., Jafari, M., Mehrabani, M., & Shakibaie, M. (2017). Microwave-assisted biosynthesis of zinc nanoparticles and their cytotoxic and antioxidant activity. *Journal of Trace Elements in Medicine and Biology, 39*, 116–123.
7. Suresh, D., Nethravathi, P. C., Udayabhanu, R. H., Nagabhushana, H., & Sharma, S. C. (2015). Green synthesis of multifunctional zinc oxide (ZnO) nanoparticles using *Cassia fistula* plant extract and

their photodegradative, antioxidant and antibacterial activities. *Materials Science in Semiconductor Processing, 31*, 446–454.
8. Azizi, S., Mohamad, R., & Shahri, M. (2017). Green microwave-assisted combustion synthesis of zinc oxide nanoparticles with *Citrullus colocynthis* (L.) Schrad: characterization and biomedical applications. *Molecules*. https://doi.org/10.3390/molecules22020301.
9. Madan, H. R., Sharma, S. C., Udayabhanu, S. D., Vidya, Y. S., Nagabhushana, H., Rajanaik, H., Anantharaju, K. S., Prashantha, S. C., & Maiya, P. S. (2016). Facile green fabrication of nanostructure ZnO plates, bullets, flower, prismatic tip, closed pine cone: their antibacterial, antioxidant, photoluminescent and photocatalytic properties. *Spectrochimica Acta Part A: Molecular and Biomolecular Spectroscopy, 152*, 404–416.
10. Kumar, R. S., Ponmozhi, M., Viswanathan, P., & Nalini, N. (2002). Effect of *Cassia auriculata* leaf extract on lipids in rats with alcoholic liver injury. *Asia Pacific Journal of Clinical Nutrition, 11*(2), 157–163.
11. Chanda, S., Kaneria, M., & Baravalia, Y. (2012). Antioxidant and antimicrobial properties of various polar solvent extracts of stem and leaves of four *Cassia* species. *African Journal of Biotechnology, 11*(10), 2490–2503.
12. Muthu, K., & Priya, S. (2017). Green synthesis, characterization and catalytic activity of silver nanoparticles using *Cassia auriculata* flower extract separated fraction. *Spectrochimica Acta Part A: Molecular and Biomolecular Spectroscopy, 179*, 66–72.
13. Padalia, H., & Chanda, S. (2017). Characterization, antifungal and cytotoxic evaluation of green synthesized zinc oxide nanoparticles using *Ziziphus nummularia* leaf extract. *Artificial Cells, Nanomedicine Biotechnology*. https://doi.org/10.1080/21691401.2017.1282868.
14. Padalia, H., Baluja, S., & Chanda, S. (2017). Effect of pH on size and antibacterial activity of *Salvadora oleoides* leaf extract-mediated synthesis of zinc oxide nanoparticles. *BioNanoScience, 7*(1), 40–49.
15. Perez, C., Paul, M., & Bazerque, P. (1990). An antibiotic assay by the agar well diffusion method. *Acta Biologiae et Medicine Experimentalis, 15*, 113–115.
16. Rakholiya, K., & Chanda, S. (2012). *In vitro* interaction of certain antimicrobial agents in combinations with plant extracts against some pathogenic bacterial strains. *Asian Pacific Journal of Tropical Biomedicine, 2*(2), 876–880.
17. Gajhiye, M., Kesharwani, J., Ingle, A., Gade, A., & Rai, M. (2009). Fungus-mediated synthesis of silver nanoparticles and their activity against pathogenic fungi in combination with fluconazole. *Nanomedicine: Nanotechnology, Biology, and Medicine, 5*, 382–386.
18. Labieniec, M., & Gabryelak, T. (2003). Effects of tannins on Chinese hamster cell line B14. *Mutation Research/Genetic Toxicology and Environmental Mutagenesis, 539*(1–2), 127–135.
19. Moteriya, P., & Chanda, S. (2016). Synthesis and characterization of silver nanoparticles using *Caesalpinia pulcherrima* flower extract and assessment of their *in vitro* antimicrobial, antioxidant, cytotoxic, and genotoxic activities. *Artificial Cells, Nanomedicine, and Biotechnology*. https://doi.org/10.1080/21691401.2016.1261871.
20. Vijayakumar, S., Vinoj, G., Malaikozhundan, B., Shanthi, S., & Vaseeharan, B. (2015). *Plectranthus amboinicus* leaf extract mediated synthesis of zinc oxide nanoparticles and its control of methicillin resistant *Staphylococcus aureus* biofilm and blood sucking mosquito larvae. *Spectrochim. Acta Part A: Molecular Biomolecular Spectroscopy, 137*, 886–891.
21. Ramesh, M., Anbuvannan, M., & Viruthagiri, G. (2015). Green synthesis of ZnO nanoparticles using *Solanum nigrum* leaf extract and their antibacterial activity. *Spectrochimica Acta Part A: Molecular and Biomolecular Spectroscopy, 136*, 864–870.
22. Awwad, A. M., Albiss, B., & Ahmad, A. L. (2014). Green synthesis, characterization and optical properties of zinc oxide nanosheets using *Olea europea* leaf extract. *Advanced Materials Letters, 5*(9), 520–524.
23. Nagajyothi, P. C., Cha, S. J., Yang, I. J., Sreekanth, T. V. M., Kim, K. J., & Shin, H. M. (2015). Antioxidant and anti-inflammatory activities of zinc oxide nanoparticles synthesized using *Polygala tenuifolia* root extract. *Journal of Photochemistry and Photobiology B: Biology, 146*, 10–17.
24. Nair, M. G., Nirmala, M., Rekha, K., & Anukaliani, A. (2011). Structural, optical, photo catalytic and antibacterial activity of ZnO and Co doped ZnO nanoparticles. *Materials Letters, 65*(12), 1797–1800.
25. Rao, V. S., Ramana, M. V., Satish, N. N., Anuradha, G., & Nageswari, B. (2013). Bio fabrication and characterization of zinc nanorods from *Aloe vera*. *International Journal of Science and Research*, 148–150.
26. Elumalai, K., & Velmurugan, S. (2015). Green synthesis, characterization and antimicrobial activities of zinc oxide nanoparticles from the leaf extract of *Azadirachta indica* (L.) *Applied Surface Science, 345*, 329–336.
27. Raj, F. A. A., & Jayalakshmy, E. (2015). Effect of zinc oxide nanoparticle produce by *Zingiber officinale* against pathogenic bacterial. *Journal of Chemical and Pharmaceutical Sciences, 8*(1), 124–127.
28. Janaki, A. C., Sailatha, E., & Gunasekaran, S. (2015). Synthesis, characteristics and antimicrobial activity of ZnO nanoparticles. *Spectrochimica Acta Part A: Molecular and Biomolecular Spectroscopy, 144*, 17–22.
29. Brayner, R., Iliou, R. F., Brivois, N., Djediat, S., Benedetti, M. F., & Fievet, F. (2006). Toxicological impact studies based on *Escherichia coli* bacteria in ultrafine ZnO nanoparticles colloidal medium. *Nano Letters, 6*(4), 866–870.
30. Baek, Y. W., & An, Y. J. (2011). Microbial toxicity of metal oxide nanoparticles (CuO, NiO, ZnO and $Sb_2O_3$) to *Escherichia coli*, *Bacillus subtilis* and *Streptococcus aureus*. *Science of the Total Environment, 409*(8), 1603–1608.
31. Sharma, S. C. (2016). ZnO nano-flowers from *Carica papaya* milk: degradation of Alizarin Red-S dye and antibacterial activity against *Pseudomonas aeruginosa* and *Staphylococcus aureus*. *Optik, 127*, 6498–6512.
32. Jayaseelan, C., Rahuman, A. A., Kirthi, A. V., Marimuthu, S., Santhoshkumar, T., Bagavan, A., Gaurav, K., Karthik, L., & Rao, K. V. B. (2012). Novel microbial route to synthesize ZnO nanoparticles using *Aeromonas hydrophila* and their activity against pathogenic bacteria and fungi. *Spectrochimica Acta Part A: Molecular and Biomolecular Spectroscopy, 90*, 78–84.
33. Banoee, M., Seif, S., Nazari, Z. E., Jafari-Fesharaki, P., Shahverdi, H. R., Moballegh, A., Moghaddam, K. M., & Shahverdi, A. R. (2010). ZnO nanoparticles enhanced antibacterial activity of ciprofloxacin against *Staphylococcus aureus* and *Escherichia coli*. *Journal of Biomedical Materials Research Part B: Applied Biomaterials, 93*(2), 557–561.
34. Dobrucka, R., & Dugaszewska, J. (2015). Biosynthesis and antibacterial activity of ZnO nanoparticles using *Trifolium pratense* flower extract. *Saudi Journal of Biological Sciences, 23*(4), 517–523.
35. Fayaz, A. M., Balaji, K., Girilal, M., Yadav, R., Kalaichelvan, P. T., & Venketesan, R. (2010). Biogenic synthesis of silver nanoparticles and their synergistic effect with antibiotics: a study against Gram positive and Gram negative bacteria. *Nanomedicine: Nanotechnology, Biology and Medicine, 6*(1), 103–109.
36. AbdElhady, M. M. (2012). Preparation and characterization of chitosan/zinc oxide nanoparticles for imparting antimicrobial and UV protection to cotton fabric. *International Journal of Carbohydrate Chemistry*. https://doi.org/10.1155/2012/840591.
37. Sharma, N., Jandaik, S., & Kumar, S. (2016). Synergistic activity of doped zinc oxide nanoparticles with antibiotics: ciprofloxacin, ampicillin, fluconazole and amphotericin B against pathogenic

microorganisms. *Anais da Academia Brasileira de Ciências, 88*(3), 1689–1698.

38. Fu, G., Vary, P. S., & Lin, C. T. (2005). Anatase $TiO_2$ nanocomposites for antimicrobial coatings. *The Journal of Physical Chemistry B, 109*(18), 8889–8898.
39. Yamamoto, O. (2001). Influence of particle size on the antimicrobial activity of zinc oxide. *International Journal of Inorganic Materials, 3*(7), 643–646.
40. Ann, L. C., Mahmud, S., Bakhori, S. K. M., Sirelkhatim, A., Mohamad, D., Hasan, H., Seeni, A., & Rahman, R. A. (2014). Antibacterial response of zinc oxide structures against *Staphylococcus aureus*, *Psuedomonas aeruginosa* and *Streptococcus pyogenes*. *Ceramics International, 40*(2), 2993–3001.
41. Chung, I. I. I.-M., Rahuman, A. A., Marimuthu, S., Kirthi, A. V., Anbarasan, K., & Rajakumar, G. (2015). An investigation of the cytotoxicity and caspase-mediated apoptotic effect of green synthesized zinc oxide nanoparticles using *Eclipta prostrata* on human liver carcinoma cells. *Nanomaterials, 5*(3), 1317–1330.
42. George, S., Pokhrel, S., Xia, T., Gilbert, B., Ji, Z., Schowalter, M., Rosenauer, A., Damoiseaux, R., Bradley, K. A., Mädler, L., & Nel, A. E. (2010). Use of a rapid cytotoxicity screening approach to engineer a safer zinc oxide nanoparticle through iron doping. *ACS Nano, 4*(1), 15–29.